

NIHAO project II: Halo shape, phase-space density and velocity distribution of dark matter in galaxy formation simulations

Iryna Butsky^{1,2*}, Andrea V. Macciò^{1†}, Aaron A. Dutton¹, Liang Wang^{3,1,4},
Greg S. Stinson¹, Camilla Penzo¹, Xi Kang³, Ben W. Keller⁵, James Wadsley⁵

¹ *Max-Planck-Institut für Astronomie, Königstuhl 17, 69117 Heidelberg, Germany*

² *California Institute of Technology, Pasadena, California, USA*

³ *Purple Mountain Observatory, the Partner Group of MPI für Astronomie, 2 West Beijing Road, Nanjing 210008, China*

⁴ *Chinese Academy of Science Graduate School*

⁵ *Department of Physics and Astronomy, McMaster University, Hamilton, Ontario L8S 4M1, Canada*

28 March 2019

ABSTRACT

We show the effect of galaxy formation on the dark matter (DM) distribution across a wide range of halo masses. We focus on how baryon physics changes the dark matter halo shape, the so called “pseudo phase-space density distribution” and the velocity distribution within the virial radius, R_{vir} and in the solar neighborhood. This study is based on the NIHAO galaxy formation simulations, a large suite of cosmological zoom-in simulations. The galaxies reproduce key properties of observed galaxies, and hence offer unique insight into how baryons change the dark matter morphology and kinematics. When compared to dark matter only simulations, the NIHAO haloes have similar shapes at R_{vir} , but are substantially rounder inside $\approx 0.1R_{\text{vir}}$. In DM-only simulations the inner halo has a minor-to-major axis ratio of $c/a \sim 0.5$. In hydro simulations c/a increases with halo mass and integrated star formation efficiency, reaching ~ 0.8 at the Milky Way mass, reconciling a long-standing conflict between observations and DM only simulations. The radial profile of the phase-space Q parameter (ρ/σ^3) is best fit with a single power law in DM-only simulations, but shows a substantial flattening within $\approx 0.1R_{\text{vir}}$ with hydro. Finally, the global velocity distribution of DM is similar in both DM-only and hydro simulations, but in the solar neighborhood, hydro galaxies deviate substantially from Maxwellian. Instead, dark matter particles show a more symmetric distribution, roughly Gaussian, around the mean, which has implications for direct DM detection experiments. Our results show that the comparison of theoretical predictions with observational data can no longer rely on pure collisionless simulations, but must include the effects of visible matter.

Key words: Galaxy: disc, evolution, structure – galaxies: disc, evolution, interactions, structure – methods: numerical, N-body simulation

1 INTRODUCTION

N-body numerical cosmological simulations have proven to be powerful tools for modeling the properties of the 3-dimensional dark matter distribution in galactic haloes (Jing & Suto 2002; Allgood 2005; Bett et al. 2007; Hayashi et al. 2007; Macciò et al. 2007; Neto et al. 2007).

However, dark-matter-only cosmological simulations only take into account the effects of gravity such that the luminous components (the stars and gas) of a galaxy evolve through cosmic time exactly like the dark matter components. However, baryons can make up a large fraction of mass in the center of galaxies, and are subject to additional hydrodynamic effects such as gas cooling and the violent explosion of stars as supernovae.

Using the Λ CDM cosmology, dark-matter-only galaxy simulations can make precise predictions of the shape and

* E-mail: ibutsky@caltech.edu

† E-mail: maccio@mpia.de

the internal matter and velocity distribution of dark matter haloes (Macciò et al. 2008). On average, such dissipationless cosmological simulations predict the ratio of the minor principal axis to the major to be $< c/a > \sim 0.6$. Observations, however, indicate that haloes are more spherical (Dubinski & Carlberg 1991). In 2001, Ibata et al. used the Sagittarius Stream to put a lower bound on the shape of the inner Milky Way halo (defined to be between 20 kpc $< r < 60$ kpc) $c/a \geq 0.8$. Other recent work found similarly spherical shapes for the inner halo of the Milky Way (Majewski et al. 2003; Helmi 2004; Martínez-Delgado et al. 2004).

In a recent, detailed study, Law & Majewski (2010) presented a new N-body model for the tidal disruption of the Sagittarius (Sgr) galaxy which led them to conclude that our Galaxy has an oblate potential with a minor to major axis ratio of $(c/a)_\phi = 0.72$. This latter value can be seen as an upper limit on the shape of the matter distribution, which again suggests a possible tension between results of pure CDM simulations and local measurements of halo shape.

One possible solution to this problem could be related to the inclusion of a dissipative component such as baryons in cosmological simulations. Katz & Gunn (1991) and Dubinski (1994) were among the first to show that haloes in dissipative simulations were systematically more spherical than corresponding haloes in dissipationless simulations. Kazantzidis et al. (2004) analyzed the effect of baryons on the shape of dark matter haloes using high resolution hydrodynamical simulations of clusters of galaxies and, again, found a reduced triaxiality in dissipational simulations. That result was confirmed in several further studies (Springel et al. 2004; Debattista et al. 2008; Pedrosa et al. 2009; Tissera et al. 2010). While there is an agreement that baryons tend to make dark matter haloes rounder, a quantitative prediction of this effect strongly depends on the prescription used to model baryons in cosmological simulations, which is not trivial task.

A large fraction of simulated galaxies used for studying the impact of baryons on the DM distribution were either plagued by the so called overcooling problem (which produced galaxies that were unrealistically dominated by baryons in their central region Kazantzidis et al. 2004) or were missing important aspects of the galaxy formation process such as star formation and feedback (Abadi et al. 2010).

A noticeable exception has been the recent work by Bryan et al. (2013), which employed the OWLs simulations (Schaye et al. 2010), a large scale simulation that produced realistic large galaxies and cosmic structure in a full cosmological framework. These simulations found that baryons substantially changed c/a of massive galaxies. On the other hand they were able to resolve galaxies on the scale of the MW with only few thousand particles.

Shape is not the only parameter of the dark matter haloes that baryons might modify. A lot of recent attention has focused on the modification of density profiles (Gnedin et al. 2004; Abadi et al. 2010; Governato et al. 2010; Macciò et al. 2012; Pontzen & Governato 2012; Di Cintio et al. 2014), which helps reduce the tension on small-scales between DM-only predictions and observations (Di Cintio et al. 2014). Another interesting quantity that is a slight variant on the density profile is the so called coarse-grained phase-space density $Q = \rho/\sigma^3$ that takes into ac-

count particle velocities as well as matter density. DM-only simulations show that radial profiles of Q are well fit with a simple power law $\rho/\sigma^3 \propto r^\alpha$ (Taylor & Navarro 2001).

Analytical work found a characteristic value for the power law slope of the Q profile, $\alpha = 1.944$, for isotropic structures (Austin et al. 2005). This value also reproduces realistic radial velocity dispersions through cosmological simulations (Dehnen & McLaughlin (2005), but see also Schmidt et al. (2008) for a more critical interpretation). It is particularly interesting to check if baryons break this simple power law behavior of the dark matter coarse-grained phase-space density in simulated galaxies.

The dark matter *velocity* distribution is another very important parameter, since it has profound implications for the the predicted dark matter - nucleon scattering rates in direct detection experiments (Kuhlen et al. 2010). Most models assume a Maxwell-Boltzmann (MB) velocity distribution function. Therefore, a departure from the MB distribution might change the predicted rate of events for dark matter models in which the scattering is sensitive to the high velocity tail of the distribution, and for experiments that require high energy recoil events (e.g. Vergados et al. 2008).

Recent high resolution DM-only simulations have reported substantial departures from a Maxwellian shape (Vogelsberger et al. 2009; Kuhlen et al. 2010), with a deficit near the peak and excess particles at high speeds. In contrast, an analysis of the *Eris* hydrodynamical simulation of a single Milky Way like galaxy, showed a different behavior. Its velocity function maintains the Maxwellian distribution and shows a greater deficit than MB at high velocities (Pillepich et al. 2012).

We revisit the issues of the effect of baryons on the dark matter properties using the galaxies from the NIHAO project (Wang et al. 2015). The NIHAO project is a large suite of high resolution simulated galaxies. The sample includes more than 65 high resolution zoom regions with halo masses ranging from 10^{10} to $Z10^{12} M_\odot$. Each high resolution galaxy is resolved with at least 400,000 elements (DM+GAS) and up to several millions (see Wang et al. 2015 for details). It is the largest sample of high resolution galaxies to date. The simulations show remarkable agreement with the stellar mass-halo mass relationship across four orders of magnitude of stellar mass. Thus a fully sampled volume would follow the observed galaxy stellar mass function. The simulations thus offer a unique tool to study the modifications that baryons induce to dark matter since it simultaneously combines high spatial and mass resolution with a statistical sample of galaxies across three orders of magnitude in halo mass.

This paper is organized as follows: in Section 2 we discuss the feedback prescription used in creating the NIHAO galaxies; In Section 3 we discuss in detail the effects of baryons on the dark matter halo shape, pseudo phase space density and the velocity distribution. Section 4 offers a summary of our results, as well as their impact.

2 SIMULATIONS

We study simulations from NIHAO project (Wang et al. 2015), that use baryonic physics from an updated

Table 1. Properties of the galaxies shown in figure 1. M_\star is the total stellar mass within R_{vir} .

Simulation name	M_\star [M_\odot]	R_{vir} [kpc]	Softening [pc]	m_{DM} [M_\odot]	m_{gas} [M_\odot]	$N_{\text{vir}}^{\text{DM}}$	$N_{\text{vir}}^{\text{gas}}$
g1.92e12	1.59e+11	281	931	1.74e+06	9.54e+04	1200667	349560
g8.26e11	4.74e+10	213	931	1.74e+06	9.53e+04	518236	255280
g7.55e11	4.50e+10	204	931	1.74e+06	9.53e+04	455930	245467
g4.99e10	1.24e+08	78	310	7.25e+04	3.97e+03	732808	154766

version of the MaGICC simulations (Stinson et al. 2013). The initial conditions are created using the latest compilation of cosmological parameters from the Planck satellite (The Planck Collaboration 2014); namely $\Omega_\Lambda = 0.6825$, $\Omega_m = 0.3175$, $H_0 = 67.1$, $\sigma_8 = 0.8344$, $n = 0.9624$ and $\Omega_b = 0.0490$. The haloes to be re-simulated with baryons and higher resolution were extracted from two different pure N-body simulations with box sizes of 60, 20 and 15 h^{-1} Mpc, more information on the DM-only simulations can be found in Dutton & Macciò (2014).

The NIHAO project was designed to study galaxy formation over a wide mass range, from dwarf galaxies to massive spirals like the Milky-Way. The simulations maintain the same *numerical resolution* across the entire mass range meaning they all have (roughly) 10^6 dark matter particles within R_{vir} . This requirement sets the mass of the dark matter particle and the initial mass of the gas particles, since the latter is simply obtained by the dark matter mass multiplied by $(\Omega_m - \Omega_b)/\Omega_b$.

The zoomed initial conditions were created using a modified version of GRAFIC2 (Bertschinger 2001; Penzo et al. 2014). The starting redshift is $z_{\text{start}} = 100$, and each halo is initially simulated at high resolution with DM-only using PKDGRAV (Stadel 2001). More details on the sample selection can be found in Wang et al. (2015). We refer to simulations with baryons as the *hydro* simulation, while we will use the term *N-body* for the DM-only simulation. Table 2 lists key properties for four galaxies across the mass range that are analyzed in more detail; the complete list of NIHAO galaxies can be found in Wang et al. (2015).

The hydro simulation is evolved using an improved version of the SPH code GASOLINE (Wadsley et al. 2004). The code includes a subgrid model for turbulent mixing of metals and energy (Wadsley et al. 2008), heating and cooling include photoelectric heating of dust grains, ultraviolet (UV) heating and ionization and cooling due to hydrogen, helium and metals (Shen et al. 2010).

For the NIHAO simulations we have used a revised treatment of hydrodynamics described in Keller et al. (2014) that we refer to as ESF-GASOLINE2. Most important is the Ritchie & Thomas (2001) force expression that improves mixing and shortens the destruction time for cold blobs (see Agertz et al. (2007)). ESF-GASOLINE2 also includes the time-step limiter suggested by Saitoh & Makino (2009), which is important in the presence of strong shocks and temperature jumps. We also increased the number of neighbor particles used in the calculation of the smoothed hydrodynamic properties from 32 to 50.

2.1 Star formation and feedback

The star formation and feedback modeling follows what was used in the MaGICC simulations (Stinson et al. 2013). Gas can form stars when it satisfies a temperature and a density threshold: $T < 15000$ K and $n_{\text{th}} > 10.3 \text{ cm}^{-3}$. Stars can feed energy back into the ISM via blast-wave supernova (SN) feedback (Stinson et al. 2006) and via ionizing radiation from massive stars before they turn in SN. Metals are produced by type II SN, type Ia SN. These, along with stellar winds from asymptotic giant branch stars also return mass to the ISM. The metals affect the cooling function (Shen et al. 2010) and diffuse between gas particles (Wadsley et al. 2008). The fraction of stellar mass that results in SN and winds is determined using the Chabrier (2003) stellar Initial Mass Function (IMF).

There are two small changes from the MaGICC simulations. The change in number of neighbors and the new combination of softening length and particle mass means the threshold for star formation increased from 9.3 to 10.3 cm^{-3} . The increased hydrodynamic mixing necessitated a small increase of pre-SN feedback efficiency, ϵ_{ESF} , from 0.1 to 0.13. This energy is ejected as thermal energy into the surrounding gas, which does not have its cooling disabled. Most of this energy is instantaneously radiated away, and the effective coupling is of the order of 1%.

3 RESULTS

To determine the properties of the dark matter halo, we considered all dark matter particles within R_{vir} (the radius that encompasses a density equal to 200 times the critical density of the Universe) found using the Amiga Halo Finder (AHF) (Knollmann & Knebe 2011). The study makes a direct comparison between the haloes that form in the DM-only simulations (black symbols in each Figure) and those that form in the hydro simulations (red symbols).

The comparison is made between all of the axis ratios (c/a), the pseudo phase space density (Q), and the velocity distribution. We investigate the velocity dispersion both globally and in the Solar neighborhood.

3.1 Halo shape

For each simulation (DM-only and hydro), we define the principal axes of the shape ellipsoid such that $a > b > c$ and define the ratio parameters, as $s = c/a$, $q = b/a$, $p = c/b$. To calculate the shape of the dark matter within a given radius, we begin with the assumption of a spherical ellipsoid, such

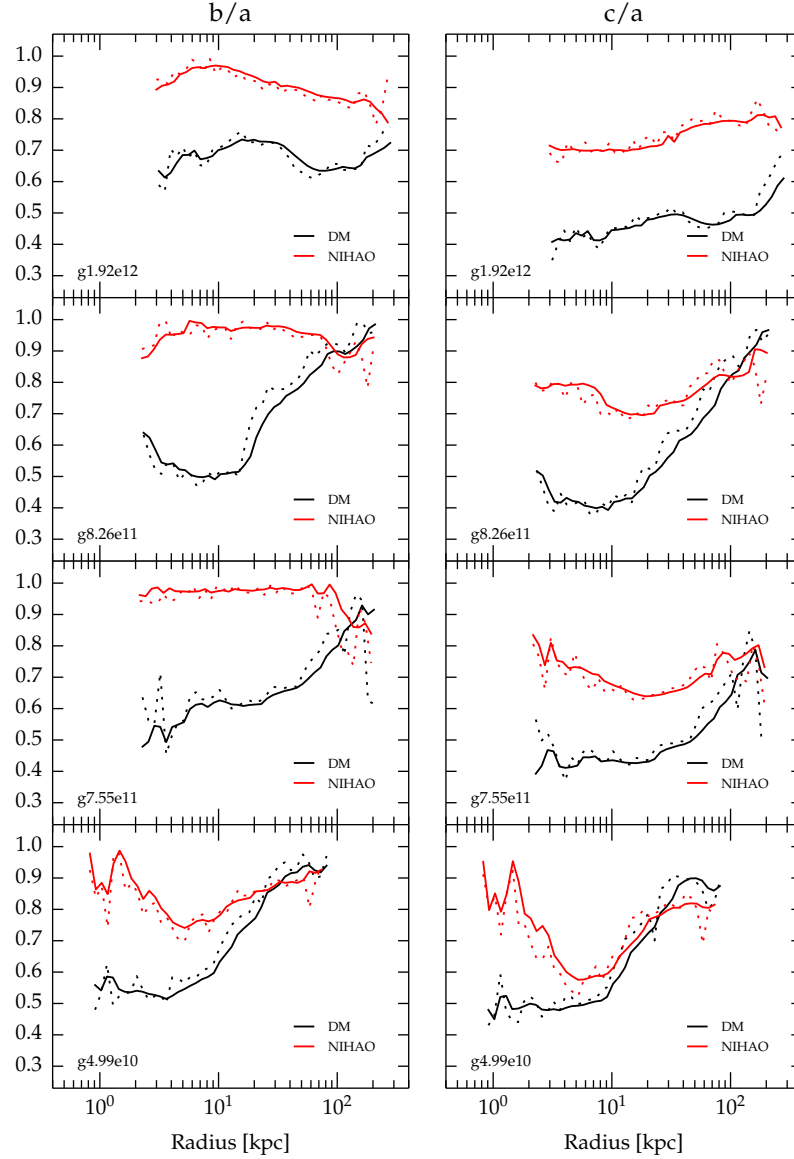


Figure 1. Ratio of middle-to-major axes (left) and minor-to-major axes (right) as a function of radius. DM simulations are depicted in black while hydro (NIHAO) simulations are depicted in red. Both the integral (solid line) and differential (dotted line) values are shown.

that $a = b = c$. We then compute the inertia tensor I_{ij} , defined as:

$$I_{ij} = \Sigma_{\alpha} m_{\alpha} x_i^{\alpha} x_j^{\alpha} / r_{\alpha}^2,$$

where m is the particle mass, α is the particle index and i, j refer to the coordinates. The radius is defined to be $r_{\alpha}^2 = x_{\alpha}^2 + y_{\alpha}^2/q^2 + z_{\alpha}^2/s^2$ (Kazantzidis et al. 2004).

The eigenvalues of this matrix produce new values for s, q, p . We iterate, using the eigenvalues of the previous matrix as the new assumptions of s and q , until the fractional difference of s, q, p converges to a tolerance value of 10^{-3} (Macciò et al. 2008).

In Figure 1, we present the relation between the middle to major axis ratio (b/a , left) and the minor to major (c/a , right) as a function of radius. The solid line is for the integral measurement of the shape (i.e. $c/a(< r)$) while the dotted line is for the differential one. In each panel the last point marks the virial radius of the halo (in this paper we define

R_{vir} as the radius that encompasses a density equal to 200 times the critical density of the Universe). For clarity and brevity we present results only four galaxies out of 67 in our sample, the total mass of each galaxy is reported in the corresponding plot.

The trend is similar across all masses: baryon physics processes such as cooling and stellar feedback modify the shape of the DM distribution. The effect of baryons physics is strongest at the center of the halo. In general, the hydro simulations maintain roughly the same shape from the center to R_{vir} . That shape is always rounder than the dark matter. At small radii, the dark matter becomes triaxial. Near R_{vir} , the shapes of the hydro and DM-only simulations converge to their most spherical shape in all the galaxies except the most massive one, g1.92e12.

The results of the dark matter halo shape at the virial radius for the whole NIHAO sample are shown in figures 2 (b/a) and 3 (c/a). At all masses the NIHAO galaxies

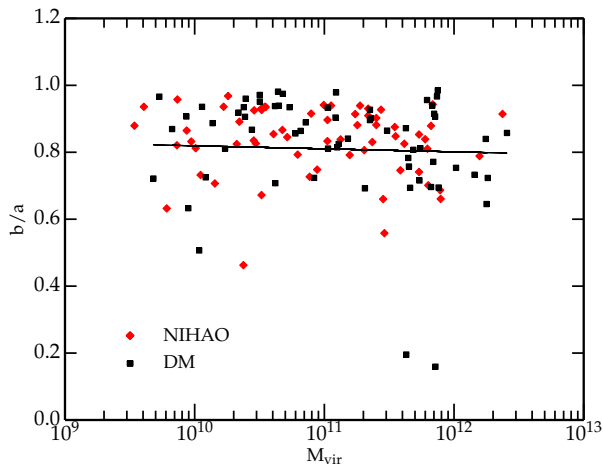


Figure 2. Ratio between the middle and the major axis of the dark matter halo (b/a) at the virial radius. The black dots represent the dark matter only simulations while the red dots stand for the NIHAO runs. The solid line shows the relation from Macciò et al. (2008).

and their pure DM counterparts show very similar values for the axis ratio, and in agreement with results obtained from larger samples of simulated dark matter haloes (Macciò et al. 2008, black solid line).

Debattista et al. (2008) described how the condensation of baryons into galaxy centers affect the dark matter shape. DM-only simulations produce haloes with a prolate shape, $\frac{1}{2}a \sim b \sim c$. Maintaining the prolate shape relies on dark matter staying on box orbits. A prime characteristics of box orbits is that they make close passages past the halo centre. As baryons cool and collapse into the centre, they deepen the potential well there and scatter material from box orbits into rounder loop or tube orbits. Tube orbits have an oblate shape, $a \sim b > c$. Fig. 1 shows the gradual transition of inner halo shapes from prolate towards oblate as the mass increases: b/a increases to 1 more quickly than c/a .

Measuring the shape of dark matter haloes at the virial radius is a quite difficult task since there are very few (if any) tracers of the DM shape (or potential) that extend so far from the galaxy center. Figures 4 and 5 show the b/a and c/a ratio measured at $0.12 \times R_{\text{vir}}$, which is in the middle of the 20-60 kpc radius range of the halo that Ibata et al. (2001) state shaped the Sagittarius stream. The steady increase of c/a (and b/a) with M_{vir} reflects the increasing efficiency of star formation with halo mass.

Fig. 6 makes the dependence of halo shape on star formation efficiency explicit. It shows the inner ($R = 0.12 \times R_{\text{vir}}$) axis ratio versus the ratio between the stellar and the total mass. Since there are no stars in the pure DM simulation we use the empirical formula of Moster et al. (2010) to assign a stellar mass to each halo (black squares).

As expected for a very low values of $M_*/M_{\text{vir}} < 0.01$ the influence of baryons is minimal and the halo shape does not change substantially between DM and hydro simulations. For larger values of the stellar-to-total mass ratio, the two distributions tend to diverge, with the NIHAO galaxies showing a substantially rounder halo shape. The shape agrees with the observations of Ibata et al. 2001 (green cir-

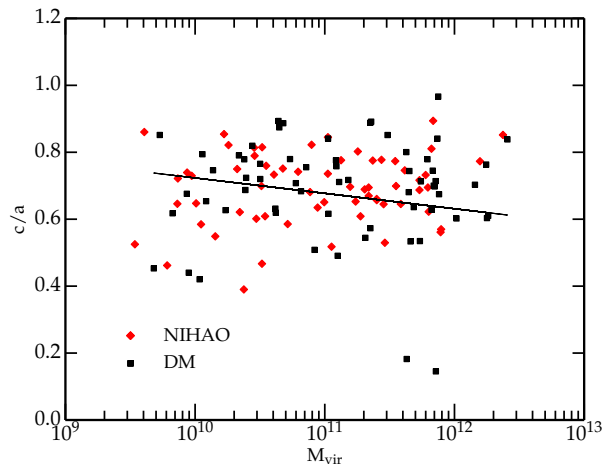


Figure 3. Ratio between the minor and the major axis of the dark matter halo at the virial radius. The black dots represent the dark matter only simulations while the red dots stand for the NIHAO runs. The solid line shows the relation from Macciò et al. (2008).

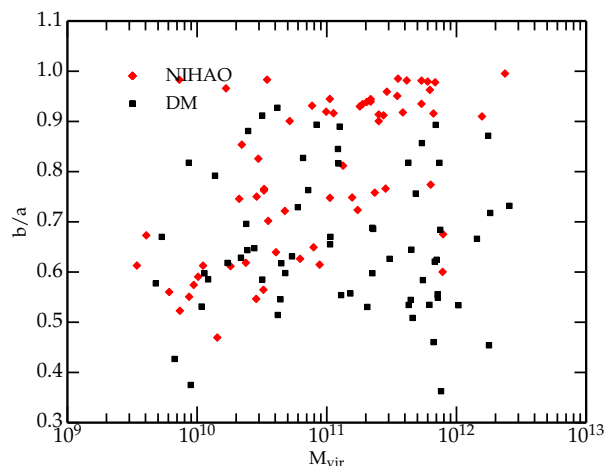


Figure 4. Ratio between the middle and the major axis of the dark matter halo (b/a) at 0.12 of R_{vir} .

cle). The behaviour of the NIHAO points is well reproduced by a simple linear fit in the log – log space:

$$\log(c/a) = A \log(M_*/M_{\text{vir}}) + B \quad (1)$$

we find the best parameters to be $A = 0.107$ and $B = -0.0087$ and the 1σ scatter around the mean to be 0.127 . The mean relation and the 1σ scatter are shown in figure 6 by the solid line and the grey area respectively.

To get an idea of whether there is a consistent shift for the inner halo shape from the DM-only to the baryon simulation, Fig. 7 shows the ratio between $(c/a)_{\text{NIHAO}}$ and $(c/a)_{\text{DM}}$ as a function of M_{vir} . The trend of halo shapes becomes more spherical with increasing halo mass is clearly visible. We decided to fit such a ratio with a simple S -shape function:

$$S(M) = s_1 + \frac{(s_2 - s_1)}{1 + (M/M_0)^\beta} \quad (2)$$

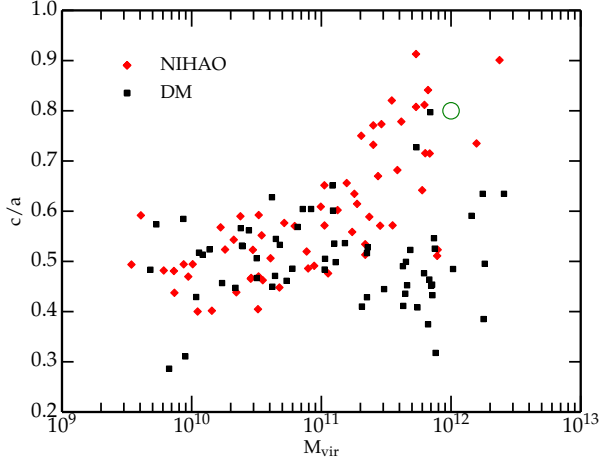


Figure 5. Same as figure 4 but for the c/a ratio. The green circle in the upper part of the plot shows the halo shape measurement for the Milky Way from Ibata et al. (2001).

Table 2. Fitting parameters describing the ratio between the DM and the hydro halo shape at 0.12 of R_{vir} .

s_1	s_2	$M_0 [M_\odot]$	β
1.848	1.0	3.1×10^{11}	1.49

where M is the virial mass of the halo. We fixed the value of the s_2 parameter to 1.0 and fit for the other ones using the Levenberg-Marquardt method, results are reported in table 3.1. The final fitting function is shown by the black line in figure 7, while the grey area represents the $1\sigma = 0.156$ scatter around the mean.

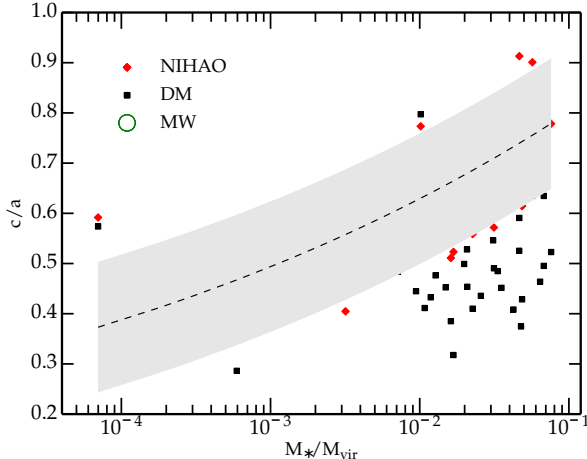


Figure 6. Shape of the inner part of the halo (0.12 of R_{vir}) vs. the star formation efficiency of the halo, parameterized as M_*/M_{vir} . The green point in the upper part of the plot shows the halo shape measurement for the Milky Way from Ibata et al. (2001). The values for M_*/M_{vir} for the DM only simulation are obtained using the relation from Moster et al (2010).

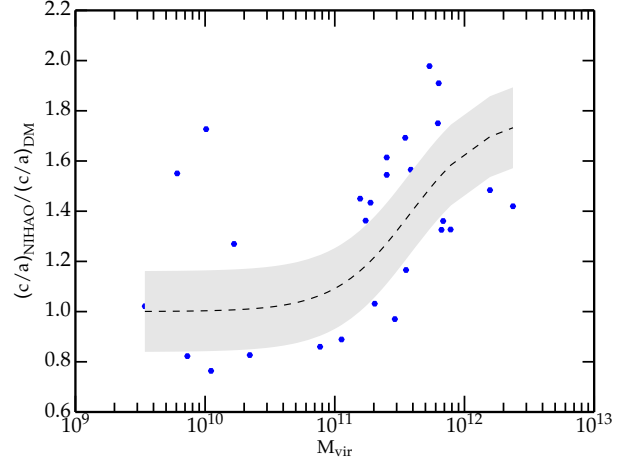


Figure 7. Ratio between the inner halo shape (c/a) in the NIHAO and DM simulations as a function of the halo mass. The dashed line is the fitting function provided in eq. 2, the grey area is the 1σ scatter around the mean.

Fig. 1 also hints that the violent motions of baryons caused by baryons in the centre of low mass galaxies also works to make the dark matter rounder. In the low mass $g4.99e10$, baryons make little change to the outer shape of the dark matter. However, the dark matter is almost completely spherical inside 2 kpc. Fig. 8 shows that is the same region in which the density profile has been flattened. It seems that the same mechanism that flattens density cusps to cores also makes the haloes round.

3.2 Dark matter pseudo phase-space density

Moving beyond the morphology of the dark matter, it is possible to also consider its kinematics. Taylor & Navarro (2001) defined “pseudo phase space density” as a simple relationship between matter density and velocity dispersion, a quantity that describes the matter distribution and kinematics of the dark matter together. They defined pseudo phase space density as:

$$Q(r) = \rho(r)/\sigma^3(r),$$

where $\sigma(r), \rho(r)$ are the velocity dispersion and density of the halo, respectively. Taylor & Navarro (2001) found that this simple combination of properties serves as a useful probe for understanding the origin of the universal DM halo profiles.

Using DM-only simulations (Taylor & Navarro 2001) found that the pseudo phase space density follows a simple power law, $Q(r) \propto r^\chi$, with $\chi \sim -1.875$. Since there is mounting evidence that baryons modify the DM density profile, $\rho(r)$, (e.g. Governato et al. 2010; Teyssier et al. 2012; Di Cintio et al. 2014, Tollet et al. 2015), it is worth checking whether baryons also reshape the Q profile.

Fig. 8 presents a comparison between the matter density profile (left) and the the pseudo phase-space density Q profile (right) for four galaxies in our sample (the same galaxies shown in figure 1). Each density profile includes three lines: the density in the pure DM simulations (black solid line), the DM density in the hydro simulations (red

solid line) and the total density profile (dark+stars+gas) in the hydro simulations (red dashed line). While profiles from DM-only simulations have universal Einasto-like shapes (e.g. Dutton & Macciò 2014), profiles from hydro simulations exhibit a core for low mass haloes which gradually steepens with halo mass, becoming even more cuspy than pure DM simulations of the most massive galaxies in our sample.

The Q profiles show a different behavior. Q in hydro simulations is always lower than its N-body counterpart. The profiles also flatten in the center even when the density profiles do not. The flattening of Q in the lowest mass halo (bottom panel) reflects the flattening of the matter density, which decreases the numerator in the definition of Q . For the other three panels, there is no such discrepancy in the matter density profile. However, the “total” density profile in the hydro simulation does get steeper in all three cases. The deeper global potential well causes the velocity dispersion of the DM σ to increase towards the center, thus flattening the inner part of the Q radial profile. As a consequence the pseudo phase-space density profile of the Dark Matter component departs from simple power law behavior at practically all mass scales probed by our hydrodynamical simulations.

3.3 Dark matter velocity distribution

As outlined in the introduction, the velocity distribution is crucial for the detection of DM in the Milky-Way. For this reason in this section we limit our analysis to galaxies with a mass similar to the one of our own Galaxy ($\approx 10^{12} M_\odot$), namely, g7.55e11, g8.26e11 and g1.92e12.

Fig. 9 shows the velocity distribution of dark matter on two different scales. The first row of Fig. 9 shows the distribution of all DM particles within the virial radius while the second row shows the distribution only inside the solar neighborhood ($7 \text{ kpc} < r < 9 \text{ kpc}$).

The black lines show results from DM-only simulations while red lines are for the NIHAO galaxies. In both types of simulations a Maxwellian distribution well represents the global velocity distribution:

$$f(x) = m_1 \frac{x^2 e^{-x^2/(2m_2^2)}}{m_2^3}. \quad (3)$$

The best fit Maxwell functions are shown as dashed lines in figure 9.

When restricted to the solar neighborhood, the DM-only and the hydro velocity distributions differ substantially in all three galaxies. The DM-only simulations can still be well fit with a Maxwellian distribution, (even if they show a slightly larger tail at high velocity). Kuhlen et al. (2010) found similar agreement using higher resolution simulations. In the hydro case, the velocity distribution is much more symmetric around the maximum value and falls quite rapidly at high velocities. As a consequence, it is better fit with a Gaussian distribution:

$$f(x) = g_1 e^{-(x-\mu)^2/(2\sigma^2)} \quad (4)$$

The Gaussian fit is shown in the lower panels of figure 9 by the (red) dotted line that clearly provides a better fit than a Maxwellian (red) dashed line. The fitting parameters for both distributions (Gaussian and Maxwellian) are reported in table 3.3.

Table 3. Parameters describing the velocity distribution function at the virial radius (first two rows) and at the solar radius (second two rows).

g7.55e11	m_1	m_2	g_1	μ	σ
R_{vir} (dm)	0.799	105.7	-	-	-
R_{vir} (hydro)	0.801	105.3	-	-	-
R_\odot (dm)	0.758	112.0	-	-	-
R_\odot (hydro)	0.834	102.9	0.0064	155.517	65.56
g8.26e11	m_1	m_2	g_1	μ	σ
R_{vir} (dm)	0.794	105.7	-	-	-
R_{vir} (hydro)	0.789	109.5	-	-	-
R_\odot (dm)	0.776	130.8	-	-	-
R_\odot (hydro)	0.903	135.5	0.0061	211.8	64.84
g1.92e12	m_1	m_2	g_1	μ	σ
R_{vir} (dm)	0.739	144.5	-	-	-
R_{vir} (hydro)	0.699	140.37	-	-	-
R_\odot (dm)	0.735	159.5	-	-	-
R_\odot (hydro)	0.969	218.0	0.0058	348.1	60.49

Our findings confirm earlier results based on the single halo ERIS simulation (Guedes et al. 2011) and presented by Pillepich et al. (2012). In their paper Pillepich and collaborators also reported a suppression of the wings and a more symmetric shape for the velocity distribution. In our simulations the differences between the pure DM case and the hydro simulations seem to be even larger. This discrepancy might be due to the stronger feedback model (which leads to a stronger baryonic impact) we have adopted in our simulations in order to balance the gas metal cooling, which was ignored in the original ERIS simulation.

As extensively discussed in Pillepich et al., the suppression of the tail of the distribution at high velocities has important consequences on the interpretation and the comparison of different direct detection experiments. For example it relaxes the tension between the (possible) signal of dark matter scattering reported by CDMS-Si (Agnese & et al. 2013) and the exclusion of such a signal from the Xenon-100 experiment (Aprile & et al. 2012). We refer the reader to Mao et al. (2014) and Pillepich et al. (2012) for a more thorough discussion.

4 CONCLUSIONS

We used the NIHAO simulation suite (Wang et al. 2015) to investigate the impact of galaxy formation on the properties of the dark matter distribution within haloes.

The NIHAO suite is a large simulation campaign aiming to produce a large sample of high resolution simulated galaxies in a cosmological context. It is an extension of the MaGICC simulations (Stinson et al. 2013) and it has been performed with an improved version of the SPH GASOLINE code (Keller et al. 2014) which fixes the well known problems of particle based hydrodynamical codes (Agertz et al. 2007). The NIHAO project counts more than 65 simulated galaxies across two orders of magnitude in halo mass ($10^{10} - 10^{12} M_\odot$), with each of the galaxies resolved with at

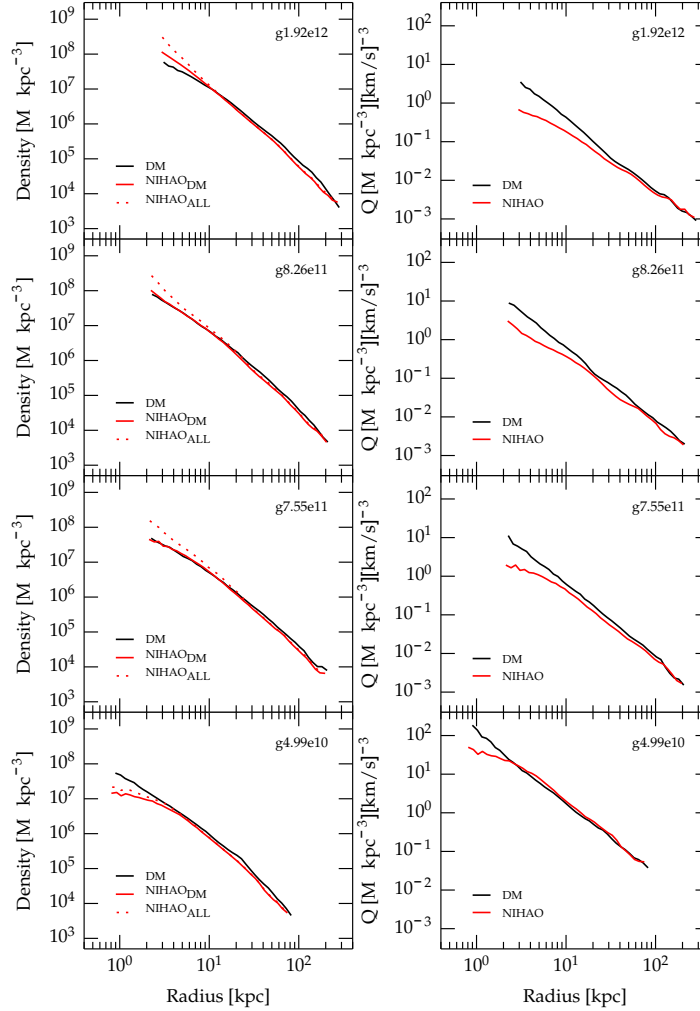


Figure 8. The density (left) and pseudo phase space density (right) of DM (black) and NIHAO (red) galaxies. Solid lines represent the density and Q values of the dark matter particles, while the dashed red line represents the total density of the star, gas, and dark matter particles.

least 4×10^5 elements. For each galaxy we have, at the same resolution, a pure N-body (collisionless) simulation and a full hydrodynamical simulation, which allows us to assess the effect of baryons on a halo-by-halo basis.

Here, we focused on three key properties of dark matter haloes: the halo shape, the radial profile of the pseudo phase-space density and the dark matter velocity distribution both global and in the solar neighborhood. Our results can be summarized as follows:

(i) The shape of the dark matter halo within the virial radius is similar between pure DM and hydro simulations. At smaller radii, however, the hydro simulations become rounder. There is a strong mass dependence to the difference between the inner halo shape (measured at 12% of the virial radius) from the pure DM simulations and hydro simulations. At low masses ($< 10^{11} M_\odot$) the dark matter halo tends to retain its original triaxial shape, while at higher masses ($\approx 10^{12} M_\odot$) the inner halo becomes more spherical with an average minor to major axis ratio (c/a) of 0.8. This brings numerical predictions into good agreement with estimates of the inner halo shape in our own Galaxy. We show that the mass dependence of the variation of

the halo shape is related to the increase of star formation efficiency with halo mass, which raises the contribution of stars and gas to the overall potential.

(ii) In hydrodynamical simulations the radial behavior of the dark matter pseudo phase space-density $Q \equiv \rho/\sigma^3$ is no longer well represented by a single power law. At all masses the Q radial profile shows a flattening towards the center of the halo. At low masses this flattening is due to the creation of a core in the dark matter potential (Tollet et al. 2015). At high masses it is due to the deepening of the total potential well which increases the velocity dispersion of the dark matter, while the density profile doesn't show large departures from the pure N-body case.

(iii) The velocity distribution of the dark matter in Milky Way-like haloes, when computed inside the virial radius, is well fitted by a Maxwellian, and it is similar to the pure DM case. But when we restrict our analysis to the solar neighborhood ($7 \text{ kpc} < r < 9 \text{ kpc}$) we find that in the hydro simulations the velocity distribution largely departs from a Maxwellian fit. It is more symmetric around the maximum and falls quite rapidly at high velocities; overall it is well fit-

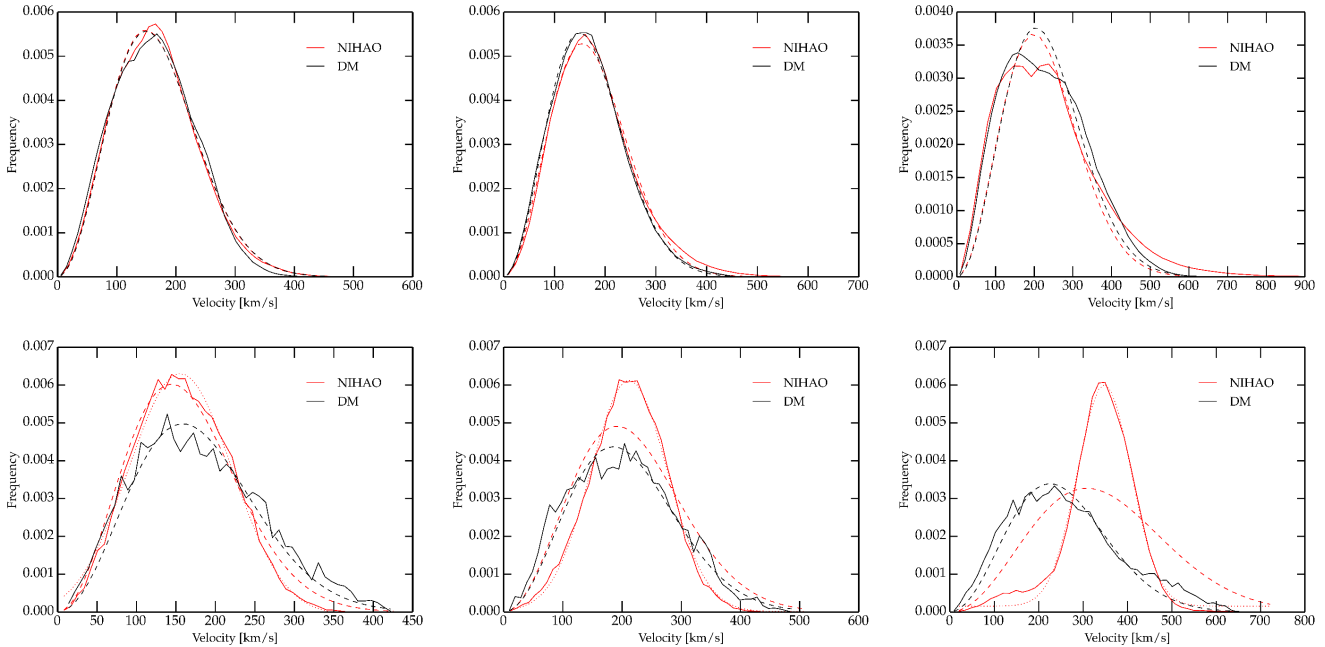


Figure 9. The velocity dispersion for g7.55e11 (left), g8.26e11 (middle), and g1.92e12 (right). The dashed lines indicate a Maxwellian fit to the simulated curves. The top panels show the global velocity dispersion, while the bottom panels show local measurements taken at the solar position. For the local velocity distribution the dotted line shows a Gaussian fit to the NIHAO curve.

ted by a Gaussian distribution. The lack of high velocity particles has important consequences for the interpretation and comparison of Dark Matter direct detection experiments.

Our results show that baryons have important effects on the dark matter not only in the very inner part (e.g. with the formation/destruction of density cores, Tollet et al. 2015) but also on the global properties of dark matter. The understanding of the nature of dark matter and the comparison of theoretical predictions with observational data can no longer rely on pure collisionless simulations, but must include the effects of visible matter.

ACKNOWLEDGMENTS

The simulations were performed on the THEO cluster of the Max Planck Institute for Astronomy, and Hydra cluster, both based at the Rechenzentrum in Garching. AVM, AAD, and GSS acknowledge support from the Sonderforschungsbereich SFB 881 “The Milky Way System” (subproject A1) of the German Research Foundation (DFG). IB contribution to this project was made possible through the SURF program at Caltech, and was supported by the Flintridge Foundation, Caltech SFP Office, and Christian Ott. IB also acknowledges support from the Sonderforschungsbereich SFB 881 “The Milky Way System” (subproject A1) of the German Research Foundation (DFG) during her stay at the MPIA. XK acknowledge the support from NSFC project No.11333008. Finally IB would like to thank Lynne Hillenbrand for her guidance in writing this paper.

REFERENCES

- Abadi M. G., Navarro J. F., Fardal M., Babul A., Steinmetz M., 2010, MNRAS, 407, 435
- Agertz O., Moore B., Stadel J., Potter D., Miniati F., Read J., Mayer L., Gawryszczak A., Kravtsov A., Nordlund Å., Pearce F., Quilis V., Rudd D., Springel V., Stone J., Tasker E., Teyssier R., Wadsley J., Walder R., 2007, MNRAS, 380, 963
- Agnese R., et al. 2013, Physical Review Letters, 111, 251301
- Allgood B. A., 2005, PhD thesis, University of California, Santa Cruz, California, USA
- Aprile E., et al. 2012, Physical Review Letters, 109, 181301
- Austin C. G., Williams L. L. R., Barnes E. I., Babul A., Dalcanton J. J., 2005, ApJ, 634, 756
- Bertschinger E., 2001, ApJS, 137, 1
- Bett P., Eke V., Frenk C. S., Jenkins A., Helly J., Navarro J., 2007, MNRAS, 376, 215
- Bryan S. E., Kay S. T., Duffy A. R., Schaye J., Dalla Vecchia C., Booth C. M., 2013, MNRAS, 429, 3316
- Chabrier G., 2003, PASP, 115, 763
- Debattista V. P., Moore B., Quinn T., Kazantzidis S., Maas R., Mayer L., Read J., Stadel J., 2008, ApJ, 681, 1076
- Dehnen W., McLaughlin D. E., 2005, MNRAS, 363, 1057
- Di Cintio A., Brook C. B., Dutton A. A., Macciò A. V., Stinson G. S., Knebe A., 2014, MNRAS, 441, 2986
- Di Cintio A., Brook C. B., Macciò A. V., Stinson G. S., Knebe A., Dutton A. A., Wadsley J., 2014, MNRAS, 437, 415
- Dubinski J., 1994, ApJ, 431, 617
- Dubinski J., Carlberg R. G., 1991, ApJ, 378, 496
- Dutton A. A., Macciò A. V., 2014, MNRAS, 441, 3359
- Gnedin O. Y., Kravtsov A. V., Klypin A. A., Nagai D.,

- 2004, *ApJ*, 616, 16
- Governato F., Brook C., Mayer L., Brooks A., Rhee G., Wadsley J., Jonsson P., Willman B., Stinson G., Quinn T., Madau P., 2010, *Nature*, 463, 203
- Guedes J., Callegari S., Madau P., Mayer L., 2011, *ApJ*, 742, 76
- Hayashi E., Navarro J. F., Springel V., 2007, *MNRAS*, 377, 50
- Helmi A., 2004, *ApJL*, 610, L97
- Jing Y. P., Suto Y., 2002, *ApJ*, 574, 538
- Katz N., Gunn J. E., 1991, *ApJ*, 377, 365
- Kazantzidis S., Kravtsov A. V., Zentner A. R., Allgood B., Nagai D., Moore B., 2004, *ApJL*, 611, L73
- Keller B. W., Wadsley J., Benincasa S. M., Couchman H. M. P., 2014, *MNRAS*, 442, 3013
- Knollmann S. R., Knebe A., , 2011, *AHF: Amiga's Halo Finder*
- Kuhlen M., Weiner N., Diemand J., Madau P., Moore B., Potter D., Stadel J., Zemp M., 2010, *Journal of Cosmology and Astroparticle Physics*, 2, 30
- Law D. R., Majewski S. R., 2010, *ApJ*, 714, 229
- Macciò A. V., Dutton A. A., van den Bosch F. C., 2008, *MNRAS*, 391, 1940
- Macciò A. V., Dutton A. A., van den Bosch F. C., Moore B., Potter D., Stadel J., 2007, *MNRAS*, 378, 55
- Macciò A. V., Stinson G., Brook C. B., Wadsley J., Couchman H. M. P., Shen S., Gibson B. K., Quinn T., 2012, *ApJL*, 744, L9
- Majewski S. R., Skrutskie M. F., Weinberg M. D., Ostriker J. C., 2003, *ApJ*, 599, 1082
- Mao Y.-Y., Strigari L. E., Wechsler R. H., 2014, *Phy.Rev.D*, 89, 063513
- Martínez-Delgado D., Gómez-Flechoso M. Á., Aparicio A., Carrera R., 2004, *ApJ*, 601, 242
- Neto A. F., Gao L., Bett P., Cole S., Navarro J. F., Frenk C. S., White S. D. M., Springel V., Jenkins A., 2007, *MNRAS*, 381, 1450
- Pedrosa S., Tissera P. B., Scannapieco C., 2009, *MNRAS*, 395, L57
- Penzo C., Macciò A. V., Casarini L., Stinson G. S., Wadsley J., 2014, *MNRAS*, 442, 176
- Pillepich A., Porciani C., Reiprich T. H., 2012, *MNRAS*, 422, 44
- Pontzen A., Governato F., 2012, *MNRAS*, 421, 3464
- Ritchie B. W., Thomas P. A., 2001, *MNRAS*, 323, 743
- Saitoh T. R., Makino J., 2009, *ApJL*, 697, L99
- Schaye J., Dalla Vecchia C., Booth C. M., Wiersma R. P. C., Theuns T., Haas M. R., Bertone S., Duffy A. R., McCarthy I. G., van de Voort F., 2010, *MNRAS*, 402, 1536
- Schmidt K. B., Hansen S. H., Macciò A. V., 2008, *ApJL*, 689, L33
- Shen S., Wadsley J., Stinson G., 2010, *MNRAS*, 407, 1581
- Springel V., White S. D. M., Hernquist L., 2004, in *Ryder S., Pisano D., Walker M., Freeman K., eds, Dark Matter in Galaxies Vol. 220 of IAU Symposium, The shapes of simulated dark matter halos.* p. 421
- Stadel J. G., 2001, PhD thesis, UNIVERSITY OF WASHINGTON
- Stinson G., Seth A., Katz N., Wadsley J., Governato F., Quinn T., 2006, *MNRAS*, 373, 1074
- Stinson G.S.and Stadel J., Maccio A., Wadsley T., Quinn T., H.M.P. C., 2013, *MNRAS*, 428, 129
- Taylor J. E., Navarro J. F., 2001, *ApJ*, 563, 483
- Teyssier M., Johnston K. V., Kuhlen M., 2012, *MNRAS*, 426, 1808
- Tissera P. B., White S. D. M., Pedrosa S., Scannapieco C., 2010, *MNRAS*, 406, 922
- Vergados J. D., Hansen S. H., Host O., 2008, *Phy.Rev.D*, 77, 023509
- Vogelsberger M., Helmi A., Springel V., White S. D. M., Wang J., Frenk C. S., Jenkins A., Ludlow A., Navarro J. F., 2009, *MNRAS*, 395, 797
- Wadsley J. W., Stadel J., Quinn T., 2004, *New Astronomy*, 9, 137
- Wadsley J. W., Veeravalli G., Couchman H. M. P., 2008, *MNRAS*, 387, 427